Levitation of cylindrical particles in the sheath of an rf plasma

B. M. Annaratone,[1,2] A. G. Khrapak,[3] A. V. Ivlev,[1,3] G. Söllner,[1] P. Bryant,[2] R. Sütterlin,[1] U. Konopka,[1] K. Yoshino,[4] M. Zuzic,[1] H. M. Thomas,[1] and G. E. Morfill[1]

[1]*Max-Planck Institut für Extraterrestrische Physik, D-85740 Garching, Germany*

[2]*Department of Engineering Science, University of Oxford, Parks Road, Oxford OX1 3PJ, United Kingdom*

[3]*High Energy Density Research Center, Russian Academy of Sciences, 127412 Moscow, Russia*

[4]*Department of Electronic Engineering, Osaka University, 565-0871 Osaka, Japan*

(Received 5 May 2000; revised manuscript received 4 October 2000; published 27 February 2001)

Microrods were levitated in the collisional sheath of a rf plasma. Rods below a critical length settle vertically, parallel to the electric field, while longer rods float horizontally. Usually rods with other inclinations spin about a vertical axis. These experimental features fit well with a model that includes a theoretical profile for the sheath, a plasma model for the screening length, which increases going deeper in the sheath, and a plasma theory for the charging of the rod's elements. Despite the agreement this paper highlights the need for a better understanding of the charging mechanism of bodies in sheaths and of the transition region in collisional sheaths.

DOI: 10.1103/PhysRevE.63.036406 PACS number(s): 52.27.Lw, 52.25.Gj, 52.35.−g

INTRODUCTION

The field of dust-plasma interaction has grown substantially in the last few years. The discovery of plasma crystallization [1] has given a tremendous stimulus to the theoretical work. In order to explain the laboratory observations ''earthly'' plasmas, the same as those used in plasma processing, have to be properly studied. These plasmas are bound by walls and subject to gravity.

One of the major tasks is to extend the theoretical work to the interaction of small bodies with the plasma sheath, the region that separates the plasma from the electrodes. In this respect the rf sheath is an interesting case [2]. rf enhanced electron currents flow to the electrodes but cannot flow in and out of the levitated particles. The case of a dc sheath around a spherical dust particle embedded in a rf enhanced plane sheath has been discussed in a number of references; see, for example, [3–5]. For small spherical bodies the interaction with the sheath is local. For elongated shapes gravity and ion drag forces must be compensated by the integral of the lifting electrostatic force over the length, in an environment where the charge and the field depend on the vertical position and where the charge and ion drag are strong functions of the inclination.

EXPERIMENTAL CONDITIONS

The experiments are performed in a GEC cell [6], in which the upper grounded electrode has been removed. The rf current flows from the driven electrode to the grounded side walls. A ring of 0.5 mm thickness and 25 mm internal diameter is placed on the driven electrode and creates a shallow electrostatic well for the levitating powder. The apparatus, the laser illumination of the dust, and the powder dispensing mechanism have already been described elsewhere [7]. Two kinds of nylon microrods of diameters 7.5 and 15 μm were levitated. These are the same rods as those levitated in dc plasma striations [8] where ordered structures of horizontally oriented particles were observed. The thinner rods consisted mostly of particles of length about 0.3 mm, with a few long ones up to 0.8 mm. The thicker rods with length up to about 0.3 mm were only few, embedded in debris that loaded the plasma and hindered a stable organization of the levitated rods.

The plasma was fully characterized using a rf filtered Langmuir probe, $r_p = 35$ μm and $l = 9.7$ mm, similar to the filtered probe described in [9]. For the analysis the cold ion radial motion theory of Allen, Boyd, and Reynolds (ABR) [10] was used to obtain the plasma density. Other quantities measured were the electron temperature and the local value of the plasma potential immediately above the levitation region.

The reasons for using radial (and not orbital) motion for the ions for finite dimensions of the probe are explained in [11,12]. The range of validity of the radial motion theory with respect to collisions is discussed in [13]. In this paper two criteria for the use of the ABR theory for the case of spherical geometry are given. The condition for the orbital motion theory to be rendered invalid by collisions is the same for spheres and cylinders:

$$\lambda < r_p \sqrt{-eV_p/kT_i}, \tag{1}$$

where λ is the mean free path or the linear dimension of the plasma, whichever is smaller, r_p is the probe radius, V_p is the probe to plasma potential, and T_i is the ion temperature. At 50 Pa the mean free path (mfp) for ion-neutral collision far from the probe (low E/p) is of the order of 0.03 mm, cross section 2.15×10^{-18} m^2 (see references in [11]). We also require collisions to be rare in the space charge region. Here the condition given in [13] is modified for cylinders as follows:

$$\lambda > 2.3 J \lambda_D . \tag{2}$$

The factor 2.3 is derived from Fig. 1 of Ref. [14], where the normalization used for the current J is given. The mfp in Eq.

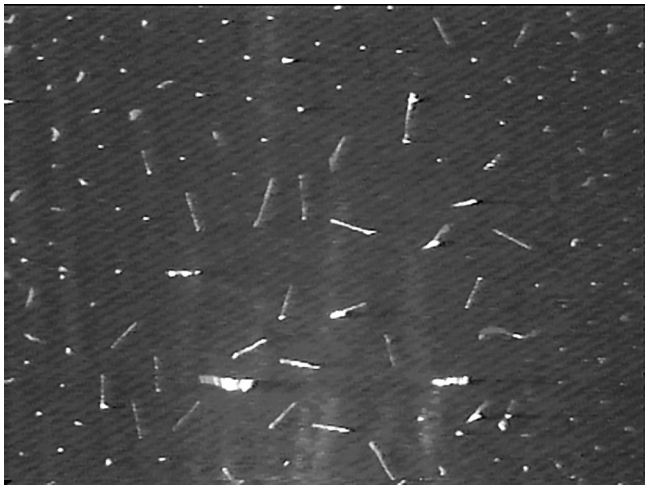

FIG. 1. The levitation of the 7.5 μm diameter rods in a krypton plasma at 52 Pa and 80 V rf as seen from the top. The dots are vertical rods.

FIG. 2. As in Fig. 1 but as seen from the side. The background shows some variation of the plasma visible emission through a 633 nm filter. On the lower left we can see the reflection from the confining rig. The region of horizontal levitation is on the right; note two horizontal particles.

(2) is somewhat longer, ≈ 1 mm, using the Cramer total cross sections [15] for ions accelerated to 5 eV, 80×10^{-20} m^2.

In our Langmuir probe measurements the plasma density as derived from the random electron current agrees well with the one derived from the ion current. This agreement excludes the possibility that the collisions could significantly perturb the radial ion motion in spite of a ratio λ_{mfp}/λ_D of the order of unity.

The dark region was evaluated by optical techniques.

EXPERIMENTAL RESULTS

A typical levitation of the 7.5 μm microrods is shown from the top in Fig. 1 and from the side in Fig. 2 in a krypton discharge with an applied rf of 80 V and a pressure of 52 Pa. Under these conditions the plasma showed increased light emission in a 3 mm thick region, adjacent to the 1.2 mm thick dark region above the driven electrode [16]. Langmuir probe characteristics taken inside the bright region show the same electron temperature as in the bulk of the discharge, with $T_e = 2.20$ eV (the high energy part of the electron energy distribution function (EEDF) is higher in the brighter plasma but this is revealed only by emission spectroscopy). The density is about 50% higher in the bright region than in the bulk, with $n_e = 3.72\times10^{15}$ m^{-3}.

Microrods longer than about 0.37 mm float horizontally mainly in the center of the area enclosed by the ring, while the shorter rods settle vertically around. The average levitation height for the vertical rods is from 1.47 to 1.84 mm above the electrode, ± 0.05 mm; the error is primarily due to the scatter of the light. The horizontal rods float near the top of the vertical ensemble in the central region and near the bottom in the vicinity of the ring (see also Fig. 2; the length of the horizontal rods cannot be derived from Fig. 2 because of the azimuthal angle). Note that the upper part of the vertical rods levitated inside the bright region.

Levitation of these rods was obtained only for discharge pressures above 5 Pa and power greater than about 20 W. Increasing the power further increased the discharge rf current but did not significantly increase the bias voltage nor did it affect the grain levitation. The kinetic energy of the ensemble, seen as spinning and random motion of the individual particles, increases with decreasing pressure because of the lower neutral gas cooling rate. This is confirmed by experiments in argon plasma, which show the same features as in the krypton plasma but with a more liquid cohesion. Another critical parameter is the amount of powder introduced. The average intergrain distance for very few vertical rods was about 1 mm; by introducing more powder the intergrain distance decreased to about 0.5 mm without changing the aggregation features, i.e., a loose hexagonal structure. When more powder was introduced the intergrain distance decreased to 0.3 mm with a clear increase of the kinetic energy. It was not possible to levitate the powder at higher densities; the excess powder just fell through.

MODEL OF THE SHEATH

The electrode sheath for pressures above 20 Pa in noble gases is highly collisional. A rough estimate of the collisionality can be derived using Cramer's total cross sections [15]. For ions accelerated to 5 eV the mean free path is about 0.1 mm, which gives 20 collisions in a 2 mm sheath. The energy acquired by an ion between two collisions is the potential difference across the sheath, about 100 eV, divided by the number of collisions. The result, 5 eV, gives an intrinsic self-consistency to the estimate. In this case a parabolic fit for the space potential is well justified by previous work, both theoretical and experimental [17].

In this paper, in order to explain the horizontal and vertical position of the rods, we will fit a parabolic potential profile that extends from the electrode to the plasma. To uniquely specify a parabola, we need three conditions. We use a coordinate system in which the zero of z, the vertical

coordinate, and of the potential are on the electrode. The first condition is the zero point. The second condition is at the visible emission boundary (z optically measured). Here the potential is the plasma potential (which when measured from the electrode is given by the dc bias plus the plasma potential, from ground, obtained by probe measurements) reduced by an average excitation energy. This is because at this energy the number of electrons able to make excited species decreases exponentially. In this work we have used as the average value for the excitation of argon 15.7 eV and for the average excitation of krypton 13.9 eV. Error can be introduced by the lifetime of the excited species. For most of the neutral excited species the lifetime is of the order of 100 ns with a thermal velocity of 268 m/s. For the ion excited species the lifetime is about 30 ns with directed velocity of the order of the Bohm speed 10^3 m/s. These excited species can emit up to 0.03 mm away from the place where they were created and this is the order of our error. The third condition is zero field in the plasma, with the plasma potential defined as above. The position of the plasma potential and the full potential profile can be derived by solving a nonlinear system.

The upper part of the levitated vertical rods lies inside the bright region and might be at the edge of the transition region. In this region a potential profile matches the sheath (where the space charge is uniform) and the presheath (which is quasineutral). In a noncollisional sheath we can distinguish between two regions, the sheath, in which a potential of the order of kT_e/e varies on distances of the order of λ_D, and a plasma part, in which a potential of $0.5kT_e/e$ (the 0.5 is for planar geometry) varies with the plasma length L. This latter potential accelerates the ions to the Bohm speed (the condition needed for a monotonic sheath). When the collision mfp is lower than L, ions entering the sheath only have the energy acquired from the last collision. An electric field is needed to accelerate the ions from the plasma to velocities comparable to the Bohm velocity against the collisional drag; hence, here the critical issue is the scale length over which the energy varies by $1kT_e$. We have now a plasma part, a transition region where the speed for entering the sheath is acquired, and the sheath. The exact shape of the transition potential is not uniquely defined. The most frequently used field, $(kT_e)/\lambda_D$ [18], is too strong and would lead to double layers. A more realistic possibility is $(kT_e)/\lambda_i$, where λ_i is the ion mean free path [19]. Other intermediate solutions are given, for example, in [20,21], and a review can be found in [22].

In our case the Blank model for the collisional sheath [21] is the most applicable and the thickness of the transition region is given by $\lambda_D^{2/3}L^{1/3}$. The field $(kT_e/e)\lambda_D^{2/3}L^{1/3}$ is lower than the field relevant for levitation. For this reason the use of the parabolic profile is fully justified.

MODEL OF CHARGING

The charge of an object imbedded in the plasma sheath of another larger body is in most cases still unknown. Experimental data are available for the charge on spherical bodies with radii on the order of micrometers [3,23]. Theories are still unsatisfactory, given that the ''isotropy'' and ''central field forces'' hypotheses, largely used in plasma theory, are not applicable here. For our purpose we have analyzed two different limiting cases, the plasma approximation and the vacuum approximation. It remains to be shown that the experimental results presented in this paper can eventually be matched by a consistent ''charging in sheath'' theory.

The plasma approximation is more justified in the upper part of the sheath where the rods settle, because here the density of the mobile charges is appreciable. In fact the density of the positive net charge in the sheath, as derived from the curvature of the potential profile, is 2.19×10^{15} m^{-3} in argon (compared to a 9.32×10^{15} m^{-3} plasma density) and 2.99×10^{15} m^{-3} in krypton (compared to a 3.72×10^{15} m^{-3} plasma density). The density of the electrons is time dependent, reaching the full plasma density in a small part of the rf cycle. The average electron density as function of the dc voltage is rf enhanced. Only the plasma model is presented in the following.

The ion flux to a cylindrical rod at 50 Pa is assumed to be radial, following the ABR theory [10] as calculated, for example, by Chen [24]. Poisson's equation in the cylindrical sheath around the rods is solved numerically using the Runge-Kutta fourth order method and the plasma solution as the boundary condition. When the ion flux is equated to the electron flux a value for the floating potential is obtained. Note that we have not introduced rf enhanced dc bias because no rf current circulates across the rod's sheath. For our purpose the calculation has been extended to a lower value of $r_p/\lambda_D=10^{-3}$, where r_p is the radius of the particle and λ_D is the electron Debye length, in order to cover the range needed for dusty plasma studies. The electric field at the probe in floating conditions is then obtained and the surface charge is derived from Gauss's law. Going vertically deeper into the electrode sheath, the screening length increases because of the reduced electron density (in Boltzmann equilibrium, the rf enhanced density). The positive screening in this kind of sheath, at least in the horizontal direction, increases with decreasing electron density. The increased screening length leads to a reduction of the floating potential down the vertical rods. Figure 3 shows the floating potential, calculated in kT_e/e units, plotted against the ratio r_p/λ_D, and Fig. 4 shows the radial electric field $d(eV/kT_e)/d(r/\lambda_D)|_{r_p}$ at the surface of the cylinder.

To derive the dimensionless charge we need to introduce a charge unit. We cannot work in analogy with the spherical case, for which the obvious choice is the vacuum capacity multiplied by kT_e/e, because the capacity per unit length of cylinders goes to infinity. Instead we assume as our charge unit the charge in a cylinder of unit length and radius λ_D of nonperturbed plasma:

$$Q_u = en\pi\lambda_D^2 l, \tag{3}$$

so that the Gauss law in dimensionless quantities (primed) is

$$Q' = 2r'E'|_{r_p',V_f'}. \tag{4}$$

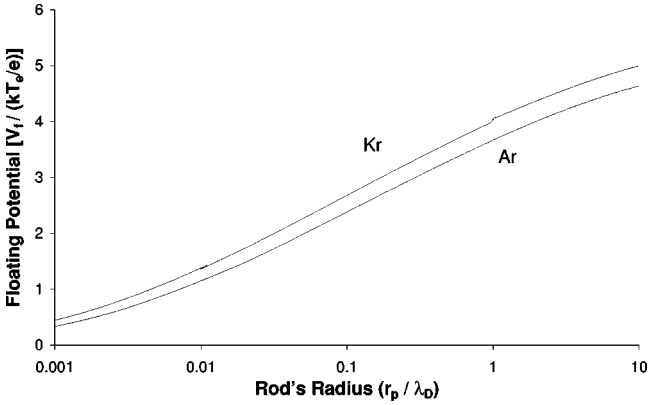

FIG. 3. The normalized floating potential for cylinders versus r_p/λ_D for argon and krypton.

See Fig. 5 for a plot of the normalized charge against the normalized radius. Figures 3–5 are published as a reference for further studies of cylindrical bodies in plasma, such as dust in microgravity plasmas or probes in rarefied laboratory plasmas.

COMPARISON OF THEORY AND EXPERIMENTS

Using the above models for the charge and for the sheath we can now calculate the lifting force for each element of surface ($r_p = 3.75\ \mu$m, $l = 10\ \mu$m) charged in the electric field of the sheath. The charge, which depends on height through the dependence on the screening length, is shown in Fig. 6, where also the electric field is shown. The force is shown in Fig. 7, where the flat straight line represents the weight of one element. The rod element is in equilibrium when the lifting force and the gravity line cross. If the same charging mechanism as in the case of vertical rods is assumed for horizontal rods, i.e., ignoring the additional charge due to the directed ion flow, two equilibria at the crossings are possible. The effect of the ion flux on horizontal rods consists in a reduced negative charge on the exposed surface, with a consequent reduction of the lifting force and decrease of the equilibrium height.

The integral of the lifting force over the rod length, with the rod placed with its top at the plasma edge, the first limit

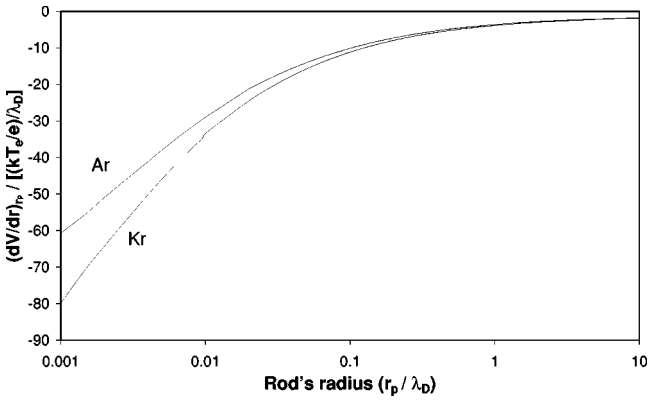

FIG. 4. The normalized electric field at the surface of a cylinder versus r_p/λ_D for argon and krypton.

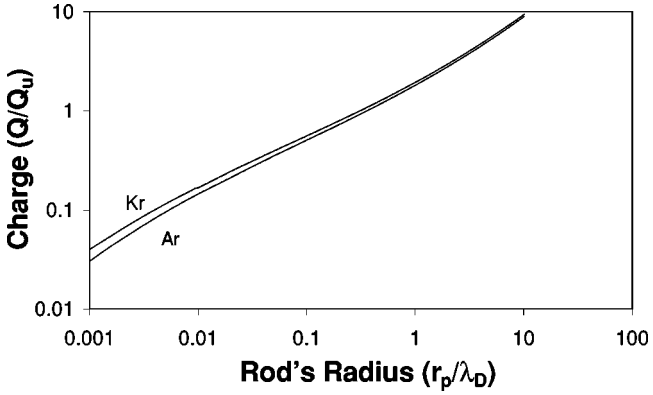

FIG. 5. The charge on a unit length cylinder, normalized to the charge inside a Debye radius and unit length cylinder of nonmodified plasma, versus r_p/λ_D for argon and krypton.

of integration, is shown in Fig. 8 for argon and krypton. Here the plasma potential is at 1.86 mm for krypton and 2.29 mm for argon. The krypton lifting force equals the gravity at 1.53 mm, predicting that 0.33 mm long rods can levitate with their tops at the plasma edge ($1.86 - 1.53 = 0.33$). This is in full agreement with the experimental data shown in Fig. 2. Note that we have not introduced any fitting parameter. As may be seen in Fig. 8, levitation with the edge of the rods at the plasma edge is forbidden in argon for any rod length. However, a range of rod sizes may be levitated in argon slightly below the plasma edge, as shown in Fig. 9. Here, the integrals of the lifting and gravity forces are calculated for rods with the height of the top as a parameter. No rods can be vertically levitated in argon below 1.6 mm, again in close agreement with the observations.

STABILITY

The stability of the rods, as a function of the inclination angle with respect to the vertical, α, is given by the simultaneous condition of vertical and rotational equilibrium:

$$\int_{z_0+(l\cos\alpha)/2}^{z_0+l(\cos\alpha)/2} F_z\,dz = 0, \tag{5}$$

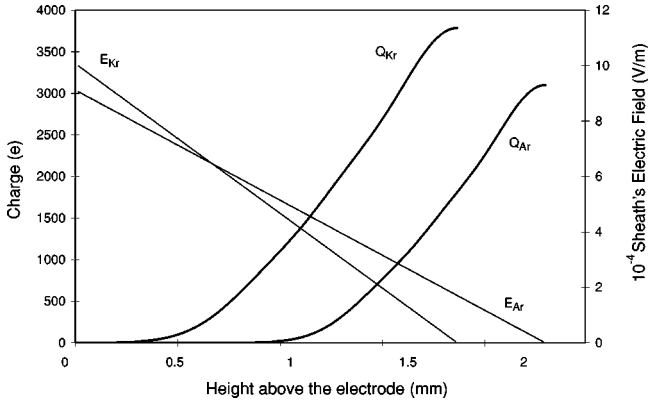

FIG. 6. The charge, in elementary charge units, acquired by a rod element of 10 μm length and 3.75 μm radius as a function of z in argon and krypton plasmas.

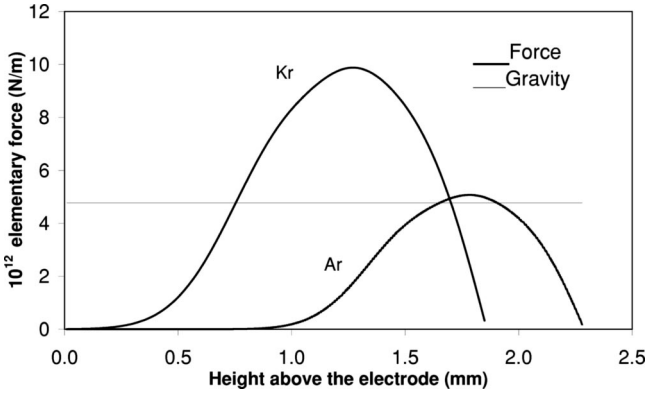

FIG. 7. The lifting and gravity force on a rod element of 10 μm length and 3.75 μm radius in argon and krypton plasmas.

$$\int_{z_0+(l\cos\alpha)/2}^{z_0+(l\cos\alpha)/2}\{F_z-\rho\Omega^2(z-z_0)\}(z-z_0)dz=0. \qquad (6)$$

Here l is the length of the rod, z_0 is the position of the center, F_z is the net vertical force, ρ is the linear density, and Ω is a possible rotation around a vertical axis. The integral of Eq. (6) has been calculated for rods near the equilibrium positions of Eq. (5) (see also Fig. 7). For the upper levitation point the torque would make a leaning rod flat because the lifting force is dominant in the lower part of the rod and the weight is dominant in the upper part. The horizontal position is then stable. This is what we see in the center of the ring, as in Fig. 1. Only the introduction of a lateral component of the electric field and/or ion drag can explain why the rods set in vertical alignment in the vicinity of the ring. The interaction energy of the crystal must also be taken into account, although the interparticle distance 0.3 mm is always larger than the screening length. The screening length ranges from 0.03 mm at the top of the vertical rod to 0.1 mm at the bottom.

For the lower equilibrium point the torque restores the vertical alignment. In fact we have observed rods nearer to the electrode to spin at a typical frequency of about 50 Hz.

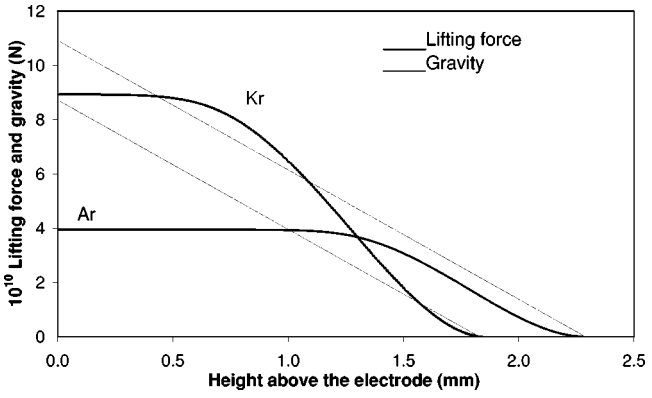

FIG. 8. The integral of the elementary lifting electrostatic force and the integral of the gravitational force, shown in Fig. 5, calculated from the upper end of the rod (at the plasma edge) to the other limit given by the difference between the plasma edge and the abscissa.

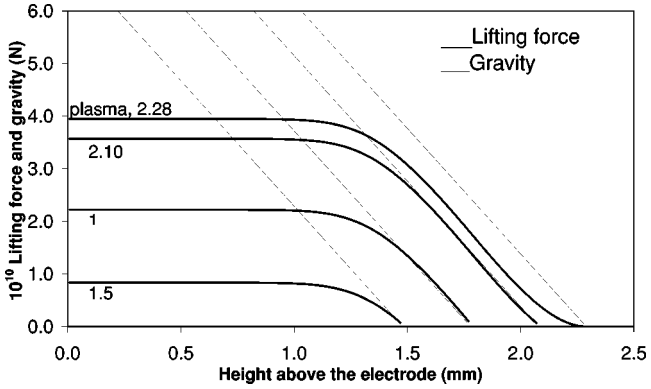

FIG. 9. As for Fig. 8 with the upper end of the rod at the specified height.

This is due to balance of the restoring torque. In krypton the first term on the left-hand side in Eq. (6) gives a torque of 5.7×10^{-15} N m when calculated on a rod 0.3 mm long, with $\alpha=45°$ in the lower equilibrium position (see Fig. 7 for f_z). This must be compared with the second term, analytically calculated, which is 5.4×10^{-15} N m for those rods spinning at 50 Hz. Some further considerations are needed for the apparent lack of damping of this motion. Without going into detail, there is evidence that energy can be supplied to the rods by the ions because of irregularity in the shapes.

CONCLUSION

Our measurements confirm that the above plasma theory could work near the top of the electrode sheath. Here we discuss some possible sources of error. (1) The electrode sheath and the particle sheath interact nonlinearly because of the presence of free charge. We have checked that the field on the rod surface is stronger than the electrode sheath field for any position on the rods. (2) The above radial motion theory for the ions assumes quasineutrality of charge at infinity while the rods lie in a positively charged environment. But in some part of the rf cycle there is quasineutrality and the electrons neutralize the ion charge on the surfaces. (3) From probe theory we know that the effect of a plasma drift on the ion current to a cylindrical body (aligned with the stream) is mainly due to end effects (see the review in [25]). In our case the effect of the higher charge of the upper end of the rod vanishes, being multiplied by an electric field that tends to zero near the plasma (an easy correction can take this effect into account when needed). (4) Errors are certainly introduced by the axial nonuniformity. In our case they might be of limited importance because the variation of the surface field along the rod's length is not more than 22%. (5) The collision ratio λ_{mfp}/λ_D is difficult to estimate because both the mfp, which is energy dependent, and the Debye length increase deep in the sheath. However, since collisions reduce the ion flux to the probe, the charge on the microrods and the floating potential will increase as a result. The charge calculated using collisionless theory is likely to be an underestimate and so should be our calculated levitation height.

Notwithstanding the uncertainty due to the above causes

we have explained the main features of the levitation of microrods in a rf plasma sheath. Among these, we have shown that rods smaller than a threshold length can levitate vertically and that horizontal rods have two equilibrium positions. We have shown that inclined rods spin in order to balance the vertically restoring torque. We also realize, of course, that the system is extremely complex and several other features still elude our understanding. In particular, we can ask why the rods need a lateral component of the electrostatic field and/or of the ion drag to lie vertically. Another question is why small rods do not lie horizontally. Perhaps end effects and/or initial boundary conditions should be investigated here. More theoretical or numerical work for the collisional rf sheath and for the transition region of increased visible emission near the electrodes, with the added complication of solution of the planar geometry, is needed for a fuller understanding.

Further work along the above lines is worthwhile. The abundance of characteristic features of the microrod systems should be exploited. For instance, filters to discriminate the particles in length and weight are obvious applications. Also, the use of spherical particles as a contactless method of diagnostics has already provided valuable information about the properties of the plasma sheath and the discharges as a whole. The use of rodlike particles expands and complements these diagnostics.

ACKNOWLEDGMENT

B.M.A. would like to acknowledge financial support from the Royal Society.

[1] H. Thomas, G. Morfill, V. Demmel, J. Goree, B. Feuerbacher, and D. Möhlmann, Phys. Rev. Lett. **73**, 652 (1994).
[2] A. Boschi and F. Magistrelli, Nuovo Cimento **29**, 487 (1963).
[3] E. Tomme, B. Annaratone, and J. Allen, Plasma Sources Sci. Technol. **9**, 87 (2000).
[4] U. Konopka, G.E. Morfill, and L. Ratke, Phys. Rev. Lett. **84**, 891 (2000).
[5] G. Morfill, H.M. Thomas, U. Konopka, and M. Zuzic, Phys. Plasmas **6**, 1769 (1999).
[6] P.J. Hargis, Jr., K.E. Greenberg, P.A. Miller, J.B. Gerardo, J.R. Torczynski, M.E. Riley, G.A. Hebner, J.R. Roberts, J.K. Olthoff, J.R. Whetstone, R.J. van Brunt, M.A. Sobolewski, H.M. Anderson, M.P. Splichal, J.L. Mock, P. Bletzinger, A. Garscadden, R.A. Gottscho, G. Selwyn, M. Dalvie, J.E. Heidenreich, J.W. Butterbaugh, M.L. Brake, M.L. Passow, J. Pender, A. Lujan, M.E. Elta, D.B. Graves, H.H. Sawin, M.J. Kushner, J.T. Verdeyen, R. Horwath, and T.R. Turner, Rev. Sci. Instrum. **65**, 140 (1994).
[7] H.M. Thomas and G.E. Morfill, J. Vac. Sci. Technol. A **14**, 501 (1996).
[8] V.I. Molotkov, A.P. Nefedov, M.Y. Pustyl'nik, V.M. Torchinsky, V.E. Fortov, A.G. Khrapak, and K. Yoshino, Zh. Éksp. Teor. Fiz. [JETP Lett. **71**, 102 (2000)].
[9] B. Annaratone and N. Braithwaite, Meas. Sci. Technol. **2**, 795 (1991).
[10] J. Allen, R. Boyd, and P. Reynolds, Proc. Phys. Soc. London, Sect. B **70**, 297 (1957).
[11] B.M. Annaratone, M.W. Allen, and J.E. Allen, J. Phys. D **25**, 417 (1992).
[12] J. Allen, B. Annaratone, and U. de Angelis, J. Plasma Phys. **63**, 299 (2000).
[13] C. Nairn, B. Annaratone, and J. Allen, Plasma Sources Sci. Technol. **7**, 478 (1998).
[14] C. Nairn, B. Annaratone, and J. Allen, Plasma Sources Sci. Technol. **4**, 416 (1995).
[15] H.W. Cramer, J. Chem. Phys. **30**, 641 (1959).
[16] S. Karderinis, D.Phil. thesis, University of Oxford, 2000.
[17] E.B. Tomme, D. Law, B. Annaratone, and J. Allen, Phys. Rev. Lett. **85**, 2518 (2000).
[18] V. Godyak and N. Sternberg, IEEE Trans. Plasma Sci. **18**, 159 (1990).
[19] T. Nitter, Plasma Sources Sci. Technol. **5**, 93 (1996).
[20] K.U. Riemann, Phys. Plasmas **4**, 4158 (1997).
[21] J.L. Blank, Phys. Fluids **11**, 1686 (1968).
[22] E. B. Tomme D.Phil. thesis, University of Oxford, 2000.
[23] U. Konopka, L. Ratke, and H.M. Thomas, Phys. Rev. Lett. **79**, 1269 (1997).
[24] F. Chen, J. Nucl. Energy, Part C **7**, 47 (1965).
[25] P. M. Chung, L. Talbot, and K. J. Touryan, *Electric Probes in Stationary and Flowing Plasmas* (Springer-Verlag, New York, 1975).